

Chapter 4

Heat balance integral method for a time - fractional Stefan problem with Robin boundary condition and temperature - dependent thermal conductivity

4.1 Introduction

The Stefan problem governing the process of heat transfer for a semi-infinite material is a moving boundary problem, which requires to determine the temperature distribution and the position of the moving phase front [3, 99, 145]. Over the past few decades, melting and freezing problems have attracted many researchers due to their nonlinear nature and extensive applications in the fields of engineering and industries. A wide bibliography related to this subject is given in [146] and a review of the analytical solutions of the classical Stefan problems is mentioned in [100, 147].

Due to the nonlinear nature of the Stefan problem, an exact solution to this type of problem is available only for a few particular cases. Therefore, we use to obtain approximate or numerical solutions for such a broad class of Stefan problems. Nowadays, there are lots of the approximate or numerical techniques available in the literature, like the Tau method [60, 85], Perturbation method [148, 134], finite

difference method [66], finite volume method [149], etc. Beside these techniques, Goodman [17] developed a popular mathematical tool, namely heat balance integral method, that specifically solves heat transfer problems during the phase change process involving a moving boundary. In this method, the heat equation is transformed into an ordinary differential equation by considering either quadratic or cubic or exponential space-dependent temperature profiles. This approximate method has been used to solve several phase change problems by assuming different types of temperature profiles [25, 29, 26, 150, 151]. In [24], various alternative avenues were established to implement the heat balance integral method. A series of papers related to the integral method has been received in the past years to solve different types of moving boundary problems and some of them can be seen in [152, 153, 154, 155]. In [156], Fabre and Hristov considered a diffusion problem with variable thermal diffusivity and derive an approximate solution by using Heat balance integral method. By using double integral balance method, an approximate solution of fractional sub-diffusional problem is given in the article of Hristov [155]. Other applications of the heat balance integral method to the non-linear heat conduction and fractional diffusion problem can be seen in [30, 157, 158, 32].

The Stefan problem governing the process of melting/solidification is commonly involved heat conduction equation, which obeys the Fourier law. Sherifi et al. [159] demonstrated that the melting process of PCM is enhanced by adding the internal horizontal rectangular fin. In [160], Shuja et al. discussed how the geometric patterns of metallic meshes enhance the melting process of phase change material. Recently, the melting inside metal foams have been also studied by Iasiello et al. [161], Sardari et al. [162] and Iasiello et al. [163]. In the last few decades, a lot of modifications have been observed in the formulation of the classical Stefan problems. In [69], Kumar and Rajeev presented a phase change problem with moving phase change material

and variable thermal conductivity. In [68], Jain et al. considered a Stefan problem with Robin boundary condition and variable thermal coefficients. In [164], Bollati and Tarzia discussed a Stefan problem with space-dependent latent heat. Many authors considered integer-order derivatives in the heat conduction equation with variable thermal coefficients and different kinds of boundary conditions in the mathematical formulations of Stefan problems [116, 46, 84, 111, 165, 88, 166]. Besides the integer-order calculus, the fractional calculus was found to be relatively flexible in the explanation of the heat conduction process [167, 168, 169, 170]. Fractional derivatives describe the memory and hereditary properties of various materials and phenomena. Therefore, many mathematical models of the Stefan problems including fractional derivatives have been received in the past decades [171, 172, 173, 174, 135]. Recently, Rajeev et al. [175] proposed an approximate solution for moving boundary problem with time-space fractional that arises in the sedimentation process. Voller [176] also studied the Stefan problem of fractional order and derived the numerical solution. Gao et al. [136] present a numerical solution of a moving boundary problem with space-fractional derivative in the field of drug release. Zheng et al. [143] also discussed a numerical solution of a time-fractional moving boundary problem. The two different fractional Stefan problems are considered by Roscani and Tarzia [177] that converge to the same Stefan problem.

Based on previous studies and observations, the time-fractional Stefan problem with variable thermal conductivity and Robin boundary condition (convective boundary condition on a fixed face) is considered. As per our knowledge, the exact solution to this problem is not available till now. Therefore, here, an approximate solution to this problem is presented by using the heat balance integral method for two different temperature profiles. To show the validation of the approximate method, the obtained results are compared with the existing analytical solution of the problem

for a particular case.

4.2 Mathematical Model

Here, a one-phase time-fractional Stefan problem in one-dimensional is considered corresponding to the melting process with temperature-dependent thermal conductivity and mixed boundary condition. The mathematical formulation of the problem is given below:

$$\rho c_0^C D_t^\alpha \theta = \frac{\partial}{\partial z} (\kappa(\theta) \frac{\partial \theta}{\partial z}), \quad t > 0, \quad 0 < z < S(t), \quad 0 < \alpha \leq 1, \quad t > 0, \quad (4.1)$$

$$\kappa(\theta(0, t)) \frac{\partial \theta}{\partial z}(0, t) = \frac{h}{t^{\alpha/2}} (\theta(0, t) - \theta_0), \quad (4.2)$$

$$\theta(S(t), t) = \theta_m, \quad (4.3)$$

$$\kappa(\theta_m) \frac{\partial \theta}{\partial z}(S(t), t) = -\rho L \frac{d^\alpha S}{dt^\alpha}, \quad (4.4)$$

$$S(0) = 0, \quad (4.5)$$

where, θ is the temperature distribution in the semi-infinite domain, κ is temperature-dependent thermal conductivity, c is the specific heat, ρ is the density, t is the time, $S(t)$ is the melting front, h is the convective heat transfer coefficient, θ_0 is the surrounding temperature of fixed face and θ_m is the melting temperature.

Here, the expression of the temperature-dependent thermal conductivity $\kappa(\theta)$ as ([84, 70]) is considered as:

$$\kappa(\theta) = \kappa_0 \left(1 + \delta \frac{\theta(z, t) - \theta_m}{\theta_0 - \theta_m} \right). \quad (4.6)$$

where κ_0 is constant thermal conductivity and $\delta \geq 0$.

4.2.1 Dimensionless form

To non-dimensionalize $\theta(z, t)$ of the model (4.1)-(4.5), the following transformation is used:

$$U(z, t) = \frac{\theta(z, t) - \theta_m}{\theta_0 - \theta_m}. \quad (4.7)$$

Using the transformation (4.7), the model (4.1)-(4.5) reduces to

$${}_0^C D_t^\alpha U = \nu \frac{\partial}{\partial z} \left((1 + \delta U(z, t)) \frac{\partial U}{\partial z} \right), \quad 0 < z < S(t), \quad 0 < \alpha \leq 1, \quad t > 0, \quad (4.8)$$

$$(1 + \delta U(0, t)) \frac{\partial U}{\partial z}(0, t) = \frac{Bi}{\sqrt{\nu t^{\alpha/2}}} (U(0, t) - 1), \quad (4.9)$$

$$U(S(t), t) = 0, \quad (4.10)$$

$$\frac{\partial U}{\partial z}(S(t), t) = -\frac{1}{\nu Ste} {}_0^C D_x^\alpha S, \quad (4.11)$$

$$S(0) = 0. \quad (4.12)$$

where $Bi = \frac{h\sqrt{\nu}}{\kappa_0}$ is the generalized Biot number (Bollati et al. (2018)), $\nu = \frac{\kappa_0}{\rho c}$ and Stefan number $Ste = \frac{c(\theta_0 - \theta_m)}{L}$.

4.3 Heat Balance Integral Method

In the heat conduction process, the fixed boundary $z = 0$ is suddenly subjected to either a fixed temperature or a flux or robin boundary condition (convective boundary condition) but, the spreading of heat into the material is not an instant process at the boundary $z = 0$. However, for $t > 0$, the spreading of heat at the boundary $z=0$ can be assumed in an interval $[0, \sigma(t)]$. In [17], Goodman developed the heat balance integral method and define a time-dependent function $\sigma(t)$, which

is assumed as the moving boundary ($S(t)$) in the case of phase change problems [150].

Therefore, integrating the heat equation Eq.(4.8) with respect to z from 0 to $S(t)$, which gives

$${}_0^C D_x^\alpha \int_0^{S(t)} U(z, t) = \nu \left(\frac{\partial U}{\partial z} \Big|_{z=S(t)} - (1 + \delta U(0, t)) \frac{\partial U}{\partial z} \Big|_{z=0} \right). \quad (4.13)$$

By using the Eq.(4.11) in Eq.(4.13), we get

$${}_0^C D_x^\alpha \int_0^{S(t)} U(z, t) = \nu \left(-\frac{1}{\nu Ste} \frac{d^\alpha S}{dt^\alpha} - (1 + \delta U(0, t)) \frac{\partial U}{\partial z} \Big|_{z=0} \right). \quad (4.14)$$

To solve the problem (4.8)-(4.12), I consider quadratic and exponential temperature profiles which are described in the following subsections:

4.3.1 Quadratic Temperature Profile

Goodman (1958) was first who applied the standard HBIM by taking quadratic profile to the phase change problem. Wood (2001) considered a different form of a quadratic temperature profile in his study. In this case, the following approximations for temperature profile and melting phase front are assumed [24]:

$$U(z, t) \approx p \left(1 - \frac{z}{S(t)} \right) + q \left(1 - \frac{z}{S(t)} \right)^2, \quad (4.15)$$

$$S(t) \approx 2\xi \sqrt{\nu t^\alpha}, \quad (4.16)$$

where $p \geq 0$, $q \geq 0$ and $\xi \geq 0$ which are determined later.

Now, we differentiate Eq. (4.15) with respect to z which give rise to the following equation for later use:

$$\frac{\partial U}{\partial z} = -\frac{p}{S} - \frac{2q}{S} \left(1 - \frac{z}{S}\right). \quad (4.17)$$

Substituting Eq.(4.15) and Eq.(4.17) in the Eq.(4.14) produces

$$\left(\frac{3p+2q}{6} + \frac{1}{Ste}\right) {}_0^C D_x^\alpha S = \nu(1 + \delta(p+q)) \frac{(p+2q)}{S}, \quad (4.18)$$

Substituting the Eqs. (4.16)-(4.17) into the Eq. (4.11) and applying the **Property 2** of Caputo derivative, we get

$$\xi = \frac{1}{2} \left(pSte \frac{\Gamma(1 - \frac{\alpha}{2})}{\Gamma(1 + \frac{\alpha}{2})} \right)^{1/2}. \quad (4.19)$$

Now, let us use Eq.(4.16) in the Eq.(4.18) which produces the following equation:

$$3(1 + \delta(p+q))(p+2q) - 6\xi^2(3p+2q) \frac{\Gamma(1 + \frac{\alpha}{2})}{\Gamma(1 - \frac{\alpha}{2})} = \frac{12\xi^2}{Ste} \frac{\Gamma(1 + \frac{\alpha}{2})}{\Gamma(1 - \frac{\alpha}{2})}. \quad (4.20)$$

With the help of Eqs.(4.15)-(4.17), the Eq.(4.9) becomes

$$(1 + \delta(p+q))(p+2q) + 2Bi\xi(p+q) = 2Bi\xi. \quad (4.21)$$

After solving the Eqs. (4.19)-(4.21), the values of p , q and ξ can be found, where ξ is a positive constant.

4.3.2 Exponential temperature profile

As given in [26], an exponential temperature profile to solve our problem (4.8)-(4.12) is taken as

$$U(z, t) = p + \frac{qz}{S} e^{-rz^2/S^2}. \quad (4.22)$$

From boundary condition (4.10) and Eq.(4.22), we get

$$U(z, t) = p(1 - \frac{z}{S} e^{r(1-z^2/S^2)}). \quad (4.23)$$

From Eq. (4.23), the derivative of $U(z, t)$ with respect to z is given by

$$\frac{\partial U}{\partial z}(z, t) = p \left(\frac{2rz^2}{S} - 1 \right) \frac{e^{r(1-\frac{z^2}{S^2})}}{S}. \quad (4.24)$$

Substituting Eq.(4.23) and Eq.(4.11) in Eq.(4.14), we get

$$\left(\frac{p(1 + 2r - e^r)}{2r} + \frac{1}{Ste} \right) S \frac{d^\alpha S}{dt^\alpha} = \nu p e^r (1 + \delta p). \quad (4.25)$$

Using the Eqs. (4.11), (4.16) and (4.24), we get

$$\xi = \frac{1}{2} \left(p(1 - 2r) Ste \frac{\Gamma(1 - \frac{\alpha}{2})}{\Gamma(1 + \frac{\alpha}{2})} \right)^{1/2}. \quad (4.26)$$

Substituting the value of $S(t)$ from Eq.(4.16) into the Eq.(4.25), we get:

$$p(1 + \delta p) e^r - \frac{4\xi^2 p(1 + 2r - e^r)}{2r} \frac{\Gamma(1 + \frac{\alpha}{2})}{\Gamma(1 - \frac{\alpha}{2})} = \frac{4\xi^2}{Ste} \frac{\Gamma(1 + \frac{\alpha}{2})}{\Gamma(1 - \frac{\alpha}{2})}. \quad (4.27)$$

Next, substituting the Eqs.(4.16), (4.23) and (4.24) into the Eq.(4.9), we have:

$$(1 + \delta p)pe^r + 2Bi\xi p = 2Bi\xi. \quad (4.28)$$

The solution of Eqs.(4.26)-(4.28) produces the values of p , r and ξ , where ξ is a positive constant.

4.4 Results and Discussion

As per our knowledge, the analytic solution of the problem (5.17)-(5.21) is not available in literature for non-zero δ . For $\delta = 0$, the following two cases are discussed:

4.4.1 Case 1: Fractional derivative

With the help of [171], it is calculated that the analytical solution of the problem (4.8)-(4.12) for a particular case ($\delta = 0$) is given by

$$U(z, t) = p_1 + q_1 \left(1 - W \left(\frac{-z}{\sqrt{\nu t^\alpha}}; -\frac{\alpha}{2}; 1 \right) \right), \quad (4.29)$$

$$S(t) = 2\xi\sqrt{\nu t^\alpha}, \quad (4.30)$$

where, p_1 , q_1 and $\xi > 0$ are constants; and the Wright function $W(x, a, b)$ is defined as

$$W(x, a, b) = \sum_{i=0}^{\infty} \frac{x^i}{\Gamma(1+a)\Gamma(ai+b)}. \quad (4.31)$$

The Eqs. (4.29)-(4.30) with the boundary conditions (4.9)-(4.11) produce the values of p_1 and q_1 as

$$p_1 = \frac{\left(1 - \left(W(-2\xi; -\frac{\alpha}{2}; 1)\right)\right)}{\left(1 + \frac{1}{Bi\Gamma(1-\frac{\alpha}{2})} - \left(W(-2\xi; -\frac{\alpha}{2}; 1)\right)\right)}, \quad (4.32)$$

$$q_1 = \frac{-1}{\left(1 + \frac{1}{Bi\Gamma(1-\frac{\alpha}{2})} - \left(W(-2\xi; -\frac{\alpha}{2}; 1)\right)\right)}, \quad (4.33)$$

and ξ can be determined by the following equation:

$$f(\xi) = \frac{\left(1 - \left(W(-2\xi; -\frac{\alpha}{2}; 1 - \frac{\alpha}{2})\right)\right)}{\left(1 + \frac{1}{Bi\Gamma(1-\frac{\alpha}{2})} - \left(W(-2\xi; -\frac{\alpha}{2}; 1)\right)\right)} - \frac{2\xi \Gamma(1 + \frac{\alpha}{2})}{Ste \Gamma(1 - \frac{\alpha}{2})} = 0. \quad (4.34)$$

4.4.2 Case 2: Integer order derivative

For $\delta = 0$, the analytic solution [100] of the problem (4.8)-(4.12) for standard case ($\alpha = 1$) is given by

$$U(z, t) = \frac{Bi\sqrt{\pi}(erf(\xi) - erf(\frac{z}{2\sqrt{vt}}))}{1 + Bi\sqrt{\pi}erf(\xi)}, \quad (4.35)$$

$$S(t) = 2\xi\sqrt{vt}, \quad (4.36)$$

where $erf(\cdot)$ is error function, Bi is Biot number and the unknown constant ξ can be determine by the following transcendental equation:

$$f(\xi) = \frac{2Bie^{-\xi^2}}{1 + Bi\sqrt{\pi}erf\xi} - \frac{2\lambda}{Ste} = 0. \quad (4.37)$$

To show the accuracy of the method, the absolute errors of the obtained results for the problem (4.8)-(4.12) are presented through the Tables 4.1 - 4.2 at $\delta = 0$. In Table 4.1, the absolute error between analytical and proposed solutions of the temperature

$(U(z, t))$ with quadratic and exponential temperature profiles is demonstrated for two different fractional order ($\alpha = 0.50, 0.75$) and standard case ($\alpha = 1$) at time $t = 10$, $Ste = 0.25$, $Bi = 0.1$ and $\nu = 1$. Comparison between the analytical and approximate solutions of the moving phase front for $Ste = 0.25$, $Bi = 0.1$, $\nu = 1$ and α ($\alpha = 0.5, 0.75, 1.0$) is shown in Table 4.2. From both the Tables 4.1 - 4.2, it is seen that the absolute errors for temperature distribution and moving phase front are nearly equal for both quadratic and exponential temperature profiles. Moreover, the proposed scheme is simple and sufficiently accurate.

The effects of fractional order (α) and various parameters on the temperature distribution and moving phase front are shown in the Figs. 4.1-4.5. Fig. 4.1 is drawn to demonstrate temperature profile for different fractional order ($\alpha = 0.25, 0.50, 0.75, 1.0$) at $t = 5$ for the parameters $Ste = 0.75$, $Bi = 0.50$, $\delta = 1$, $\nu = 1$. Fig. 4.2 depicts the impact of fractional order ($\alpha = 0.25, 0.50, 0.75, 1.0$) on the tracking of moving phase front ($S(t)$) for parameters $Ste = 0.75$, $Bi = 0.50$, $\delta = 1$, $\nu = 1$. In case of variable thermal conductivity, Figs. 4.1-4.2 show that the temperature profile and trajectory of moving phase front shift towards the standard case ($\alpha = 1$) as we increase the values of α . This observation is similar to the results obtained in the case of constant thermal conductivity [134]. In Fig. 4.2, the movement of phase front is slower for large value of α for a short time. After that the movement of phase front becomes fast as we increase the value of α . This leads overlapping of curves in the figure. Fig. 4.3 is plotted to show the effect of Biot number (Bi) on the temperature distribution for $Ste = 0.75$, $\delta = 1$ and $\nu = 1$ at time $t = 5$. For fractional case ($\alpha = 3/5$), it is observed from Fig. 4.3 that the temperature at the first boundary as well as the rate of temperature distribution with respect to z enhance with the increment of Biot number. The variation of location of moving phase front with respect to the Biot number is demonstrated for the fixed

parameters $Ste = 0.75$, $\delta = 1$ and $\nu = 1$ in Fig. 4.4. This figure shows that the melting front ($S(t)$) moves faster when we increase the values of Biot number for fractional order derivative ($\alpha = 3/5$). The results of Figs. 4.3-4.4 for fractional case are similar to the standard case [87]. The impact of the parameter δ on the moving melting front ($s(t)$) is presented in Fig. 4.5 at $Ste = 0.50$, $Bi = 1$ and $\nu = 1$ for the fractional derivative ($\alpha = 1/2$). From the Fig. 4.5, it is observed that the melting front moves faster when we increase δ , hence the melting process accelerates. But, the effect of Bi on the development of the melting front is more pronounced than δ .

TABLE 4.1: Absolute errors of approximated temperature distribution ($U(z, t)$) at $t = 10$.

<i>S.No.</i>	α	z	Absolute Error in quadratic temperature profile	Absolute Error in exponential temperature profile
1	0.50	0.00	1.10139×10^{-4}	1.10371×10^{-4}
		0.01	1.09132×10^{-4}	1.09347×10^{-4}
		0.02	1.05992×10^{-4}	1.06163×10^{-4}
		0.03	1.00722×10^{-4}	1.00837×10^{-4}
		0.04	9.33306×10^{-5}	9.33898×10^{-5}
		0.05	8.38236×10^{-5}	8.38396×10^{-5}
2	0.75	0.00	9.04124×10^{-5}	9.07426×10^{-5}
		0.01	9.01109×10^{-5}	9.04309×10^{-5}
		0.02	8.91294×10^{-5}	8.94219×10^{-5}
		0.03	8.74666×10^{-5}	8.77189×10^{-5}
		0.04	8.51214×10^{-5}	8.53252×10^{-5}
		0.05	8.20925×10^{-5}	8.22444×10^{-5}
3	1.00	0.00	5.03897×10^{-7}	5.53845×10^{-11}
		0.01	4.98137×10^{-7}	5.53661×10^{-11}
		0.02	4.81586×10^{-7}	5.51343×10^{-11}
		0.03	4.55818×10^{-7}	5.44860×10^{-11}
		0.04	4.22406×10^{-7}	5.32394×10^{-11}
		0.05	3.82923×10^{-7}	5.12439×10^{-11}

TABLE 4.2: Absolute errors of approximated moving phase front $S(t)$.

$S.No.$	α	t	Absolute Error in Quadratic temperature profile	Absolute Error in Exponential temperature profile
1	0.50	0.1	4.17787×10^{-4}	4.17782×10^{-4}
		0.2	4.96835×10^{-4}	4.96829×10^{-4}
		0.3	5.49838×10^{-4}	5.49832×10^{-4}
		0.4	5.90839×10^{-4}	5.90833×10^{-4}
		0.5	6.24737×10^{-4}	6.24729×10^{-4}
2	0.75	0.1	2.57318×10^{-4}	2.57311×10^{-4}
		0.2	3.33699×10^{-4}	3.33692×10^{-4}
		0.3	3.88499×10^{-4}	3.88489×10^{-4}
		0.4	4.32755×10^{-4}	4.32744×10^{-4}
		0.5	4.70526×10^{-4}	4.70514×10^{-4}
3	1.00	0.1	8.95202×10^{-9}	1.01143×10^{-12}
		0.2	1.26601×10^{-8}	1.43037×10^{-12}
		0.3	1.55053×10^{-8}	1.75184×10^{-12}
		0.4	1.79040×10^{-8}	2.02285×10^{-12}
		0.5	2.00173×10^{-8}	2.26161×10^{-12}

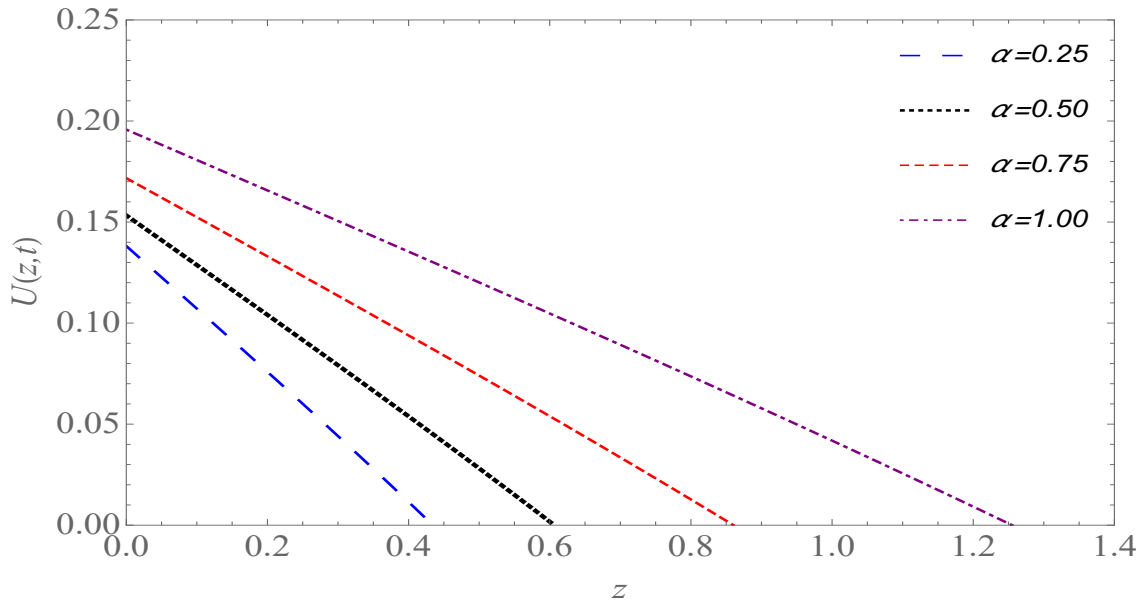


FIGURE 4.1: Effect of the fractional order α on temperature profile ($U(z, t)$) at $t = 5$.

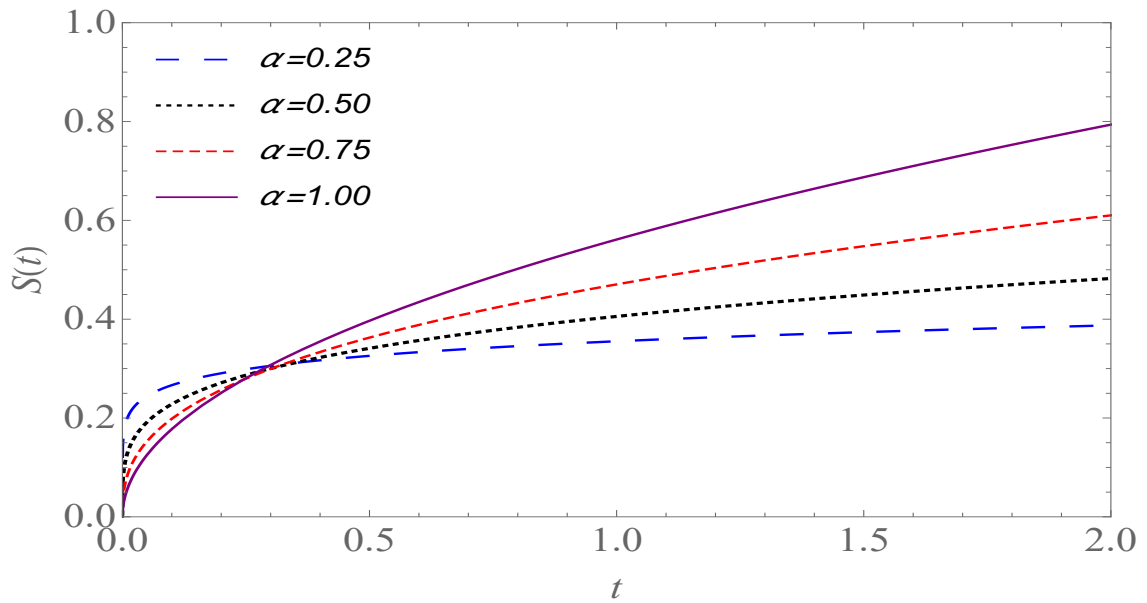


FIGURE 4.2: Effect of the fractional order α on moving phase front ($S(t)$).

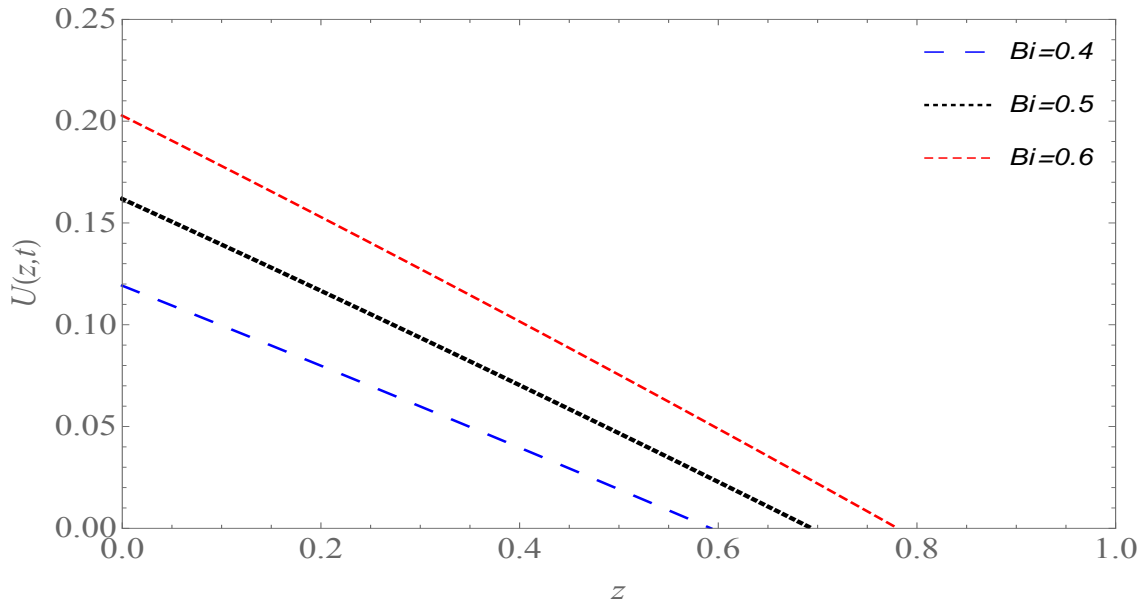


FIGURE 4.3: Impact of Bi on the temperature profile at $t = 5$ and $\alpha = 3/5$.

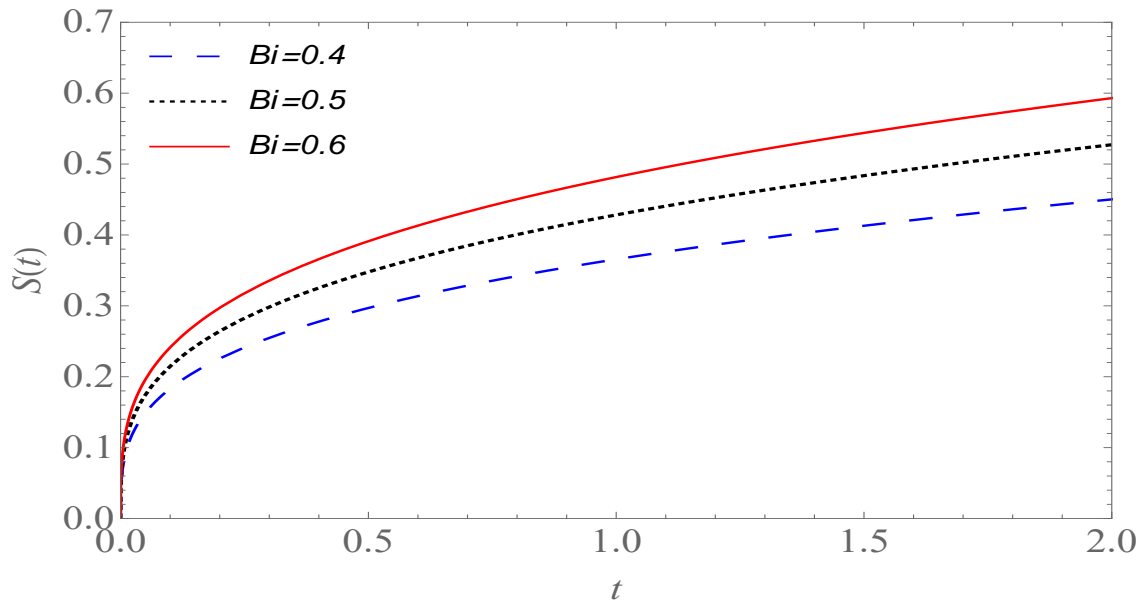


FIGURE 4.4: Impact of Bi on the moving phase front ($S(t)$) at $\alpha = 3/5$.

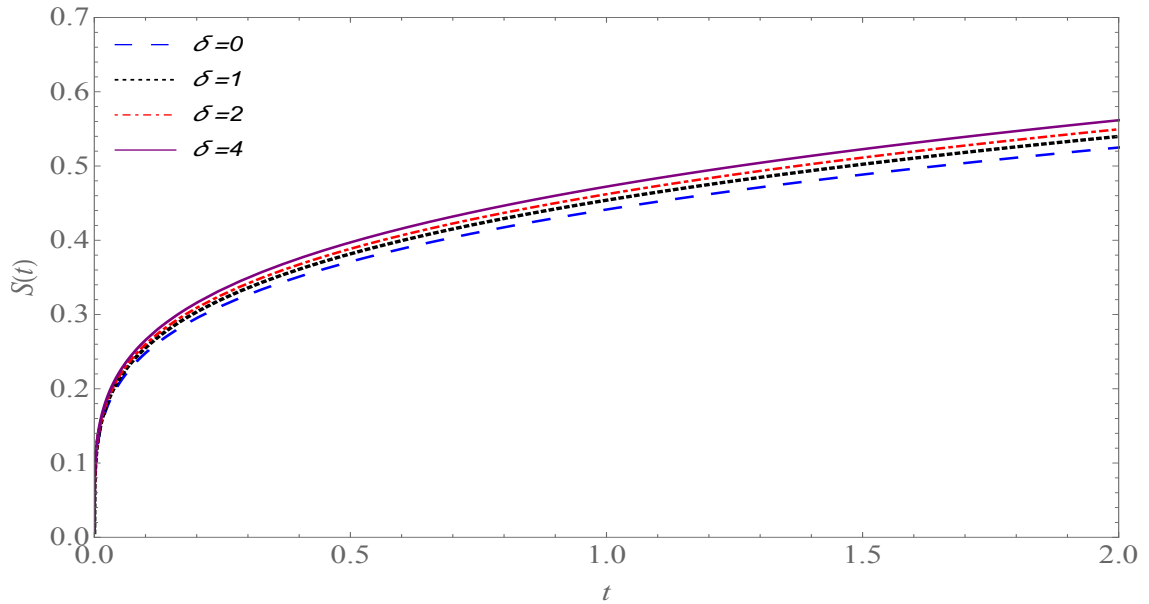


FIGURE 4.5: Effect of δ on the moving phase front ($S(t)$) at $\alpha = 1/2$.

4.5 Conclusion

In this chapter, the heat balance integral method is successfully applied for quadratic and exponential temperature profiles to present an approximate solution of a time fractional Stefan problem with mixed boundary condition and variable thermal conductivity. From this study, it is observed that this approximate technique is accurate and efficient method for the solution of wide class Stefan problem. Moreover, the solution of the problem obtained by quadratic and exponential approximations are nearly equal for the fractional case, but the exponential approximation provides more accurate result than the quadratic approximation for standard case. It is also seen that the fractional order α affects the tracking of the melting front and melting process. The melting process becomes fast as we increase the fractional order α after a short time interval but the reverse trend is seen initially. Biot number Bi

and δ also influence the melting process for fractional case and it is observed that the process grows faster when we increase the Bi and δ .
